COMPDYN 2013
4th ECCOMAS Thematic Conference on
Computational Methods in Structural Dynamics and Earthquake Engineering
M. Papadrakakis, V. Papadopoulos, V. Plevris (eds.)
Kos Island, Greece, 12–14 June 2013

ENVELOPE PRINCIPLE IN MULTI-MODE PUSHOVER PROCEDURE FOR RC BUILDINGS

Ante Mihanović[1], Ivan Balić[1], Boris Trogrlić[1]
[1] University of Split, Faculty of Civil Engineering, Architecture and Geodesy
Matice hrvatske 15, 21000 Split, Croatia
boris.trogrlic@gradst.hr

Keywords: Multi-mode pushover, Target acceleration, Envelope, RC frames.

Abstract. *Pushover method is a practical procedure for comprehensive nonlinear analysis of structures subjected to seismic action. Application of this method, in accordance with the Eurocode 8 rules and due to engineering simplicity, favours application utilizing the first mode. Aim of research presented in this paper was to find the influence of multimodal combinations in assessing the bearing capacity of reinforced concrete (RC) frames and walls. This paper presents a procedure in which the most extreme state is defined by the lowest ground acceleration caused by a predetermined shape of an elastic spectrum. Extreme bearing value is obtained by the envelope principle. Mode shapes and period sizes are determined on a linear elastic model while the limit state of the load bearing system is evaluated in a nonlinear state of structures. Results of the analysis show that influences of higher modes are significantly bigger and that the safety/reliability, indicated by criteria for the target displacement, in accordance with Eurocode 8 (Annex B), is not achieved. Inclusion of higher modes, in some presented examples, decreases the limit ground acceleration by more than two times, which is significantly less favourable than the target displacement criteria.*

1 INTRODUCTION

A multi-mode pushover procedure for comprehensive nonlinear static analysis of structures subjected to seismic action is presented in paper. When combined with response spectrum of a single degree of freedom system it gives the assessment of bearing capacity and deformation of structures during earthquakes.

Pushover procedure is implemented in many international codes for design of structures, as well as recommended provisions of research institutions [1-3]. Development of procedure implemented in Eurocode 8 started three decades ago [4-6], while numerous improvements and applications [7, 8] are still current [9]. In practical application, pushover method based on linear or constant distribution of acceleration, is dominant. In numerous research papers, such as [10-16] influence of higher modes on the results of nonlinear static analysis applied through the pushover method were analysed with the conclusion of significant impact of higher modes.

This paper presents the approach of inclusion of higher modes through trial method in order to satisfy the envelope method. Method can be applied only on a specific elastic spectrum. In examples presented in this paper, spectrum type *1* and ground type *A* is chosen in accordance with the Eurocode 8.

Capacity curves are determined by pushover analysis, and then converted in ADRS (Acceleration-Displacement Response Spectrum) format according to previously selected spectrum for the first few modes. Input data for modal load vectors are determined based on linear elastic analysis.

Now, trial method can be applied by the trial principle as follows:

- Hypothetic acceleration is selected and joint to previously selected specific elastic spectrum.
- For each mode separately, based on capacity curve, corresponding level of spectral acceleration and spectral force must be determined taking into account target displacement according to Eurocode 8. Distribution of acceleration, i.e. shape of load vector, corresponds to the shape of the corresponding mode.
- Furthermore, general load vector must be formed as a load vector, according to some of possible combination of actual modes. As possible combinations, this paper analysed: linear combination (L) and square root of sum of square combination (SRSS).
- For thus formed total load vector on structure (starting load), bearing capacity of structures, i.e. computational limit load, is determined by nonlinear static analysis.

Solution is considered to be the one in which, within the limits of calculation accuracy, a computational limit load from ultimate limit state is equal to starting load from assumed ground acceleration. In couple selection attempts of various hypothetic acceleration and corresponding vectors, procedure leads to a solution quickly. Obtained solution gives us the *target acceleration*. It represents the lowest acceleration which, according to nonlinear static analysis and multi-mode analysis, leads to computation limit state.

Based on processed examples of linear and SRSS combinations it was logical to conclude that target acceleration must be lower than acceleration belonging to specific mode. That fact presents initial step in this trial method. Final solution has all the characteristics of an envelope principle.

2 TARGET ACCELERATION DETERMINATION

Procedure of target acceleration determination begins by determining structure's modes $\boldsymbol{\phi}_i$, corresponding periods T_i and modal masses m_{ei}, all based on linear elastic analysis. Load vector for each specific i-th mode $\boldsymbol{F}_i$ is determined by the intensity factor of total load p_i, as well as the product of diagonal mass matrix $\boldsymbol{M}$ and mode $\boldsymbol{\phi}_i$.

$$\boldsymbol{F}_i = p_i \, \boldsymbol{M} \, \phi_i \tag{1}$$

Capacity curves are calculated by material and geometric nonlinear numerical model [17] with monotonic increase of each load vector $\boldsymbol{F}_i$. This way, failure lateral forces in the base of model F_{fi} is obtained for each specific load vector.

In searching for target acceleration, each attempt starts with assumed value of target ground acceleration a_{gr}. For assumed a_{gr}, type of elastic spectrum (type *1* or type *2*), ground type (soil factor S) and damping correction factor (η=1 for ξ=5% viscous damping ratio), an ADRS curve is constructed. In that ADRS curve a capacity curve is embedded which is obtained for each specific load factor.

Spectral acceleration $a_{s,i}$ is obtained for each mode independently, in accordance with Eurocode 8 and Annex B, choosing that displacement on capacity curve at failure is 150% of target displacement, or

$$d_t = \frac{2}{3} d_u \tag{2}$$

Thereby, corresponding bilinear force-deformation diagram must be found, i.e. diagram where intersection of period T_i and related target displacement d_t exist on ADRS curve created for assumed ground acceleration. In other words, equality of obtained ground acceleration $a_{gr,i}$ in i-th attempt with assumed ground acceleration a_{gr} must be found, from which spectral acceleration $a_{s,i}$ will follow. Search procedure for corresponding bilinear force-deformation diagram is shown in Figure 1.

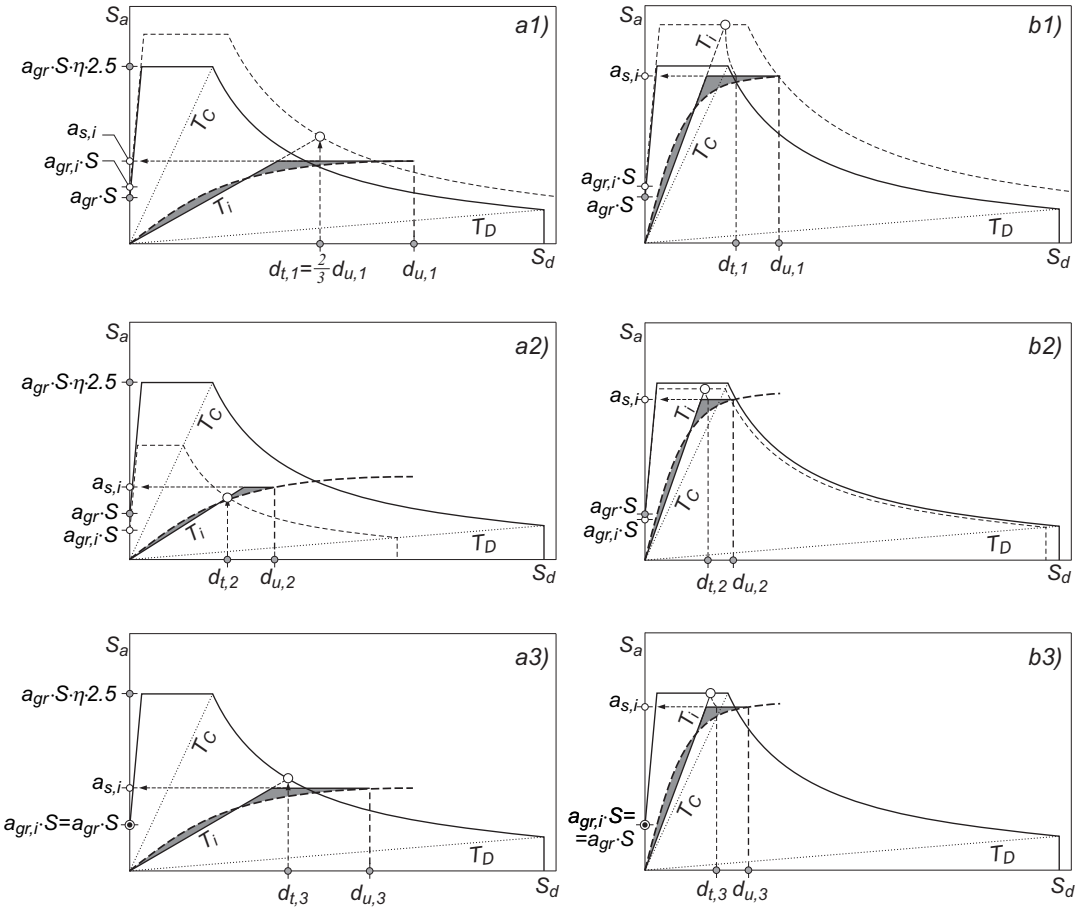

Figure 1: Spectral acceleration determination $a_{s,i}$: a1)-a3) for $T_i \geq T_C$; b1)-b3) for $T_i < T_C$.

In the case when the period is $T_i \geq T_C$, in Figures 1.a1) and 1.a2) chosen bilinear force-deformation diagrams are presented. In Figure 1.a1) chosen diagram gives bigger and on Figure 1.a2) lower ADRS curve ordinates than ADRS curve of assumed ground acceleration a_{gr}. In Figure 1.a3) chosen diagram for corresponding period T_i and related target displacement d_t gives intersection on ADRS curve, from which follows spectral acceleration $a_{s,i}$. Similar procedures have to be performed in case of $T_i < T_C$ when searching for intersection according to path defined by Eurocode 8 - Annex B.

After this is performed, for each vector, parameter δ should be defined, as a ratio between accordingly obtained spectral acceleration and assumed ground acceleration

$$\delta_i = \frac{a_{s,i}}{a_{gr}} = \delta_i\left(a_{gr}\right) \tag{3}$$

Hereafter, some modal combinations are defined. It is standard to use linear combination (L) and square root of sum of square combination (SRSS). Target acceleration result is obtained by applying successive attempts, varying assumed acceleration as initial data.

2.1 Target acceleration at linear combination of modes

Shape of the starting hypothetic vector of limit load $\boldsymbol{F}_L$ for linear combination is defined as

$$\sum F_i = \sum \pm\, m_{ei}\, \delta_i\, F_{fi} \tag{4}$$

where sign ± means more unfavourable influence on the characteristic section. Characteristic section, here presented on a specific example (RC frame), is a sum of bending moments at the bottom of the first floor. During the selection of the algebraic sign, group influence line for characteristic values can be used.

In numerical procedure, proposed loading is applied incrementally. As a result, associated computation limit loading is obtained, i.e. force in basis of model F_f.

Ratio between starting hypothetic vector F_L and computational limit load F_f shows the reality of the starting assumption. Only when aforementioned equality is obtained, within the limits of computational accuracy, required result is achieved; extreme, i.e. the lowest limit ground acceleration, named target acceleration $a_{gr,t}$.

2.2 Target acceleration according to SRSS modal combination

Square root of sum of square modal combination is a method which can be simplified, in case when the first mode is dominant, as a sum of the first member and half of other members. Half of participating loading of higher individual mode is approximately equal to total loading belonging to the spectrum with acceleration of $a_{gr}/2$ [18], so appropriate combination may be defined as

$$\sum F_i = \pm m_{e1}\, \delta_1\left(a_{gr}\right) F_{\underset{1}{f}} + \sum_{i=2}^{n} \pm\, m_{ei}\, \delta_i\left(a_{gr}/2\right) F_{fi} \tag{5}$$

Rest of the procedure is analogue to procedure described for linear combination.

3 EXAMPLE

Hereafter, example of 9-storey space reinforced concrete frame is analysed. Calculation is performed taking into account the following assumptions and limitations: (i) calculation of dynamic properties (ϕ_i, T_i, m_{ei}) is conducted on a linear model of RC frame with floor slabs

and with initial modulus of elasticity E_0; (ii) torsion effects are not included in the calculation; (iii) frames from both examples are symmetric around two axis.

3.1 Model description and calculation of loading vector

The 9-storey space RC frame, with dimensions shown in Figure 2a, is analysed. Dimensions and discretization of cross sections of beams are shown in Figures 2d and 2e, and dimensions and discretization of cross sections of columns are shown on Figure 2f. Properties of cross sections are assigned to frame according to Figure 2c. Distributed loading is assigned on beams according to Figure 2b, and concentrated forces are set in nodes on intersections of beams and columns. For computation of eigenvectors a concentrated mass is assigned (Figure 2b) and material modulus E=24.38 GPa, as initial elastic modulus of concrete. To calculate the capacity curve, numerical models of concrete and steel are used as shown in Figure 2g. Total weight of model is W=14903 kN, i.e. M=1519.2 tons.

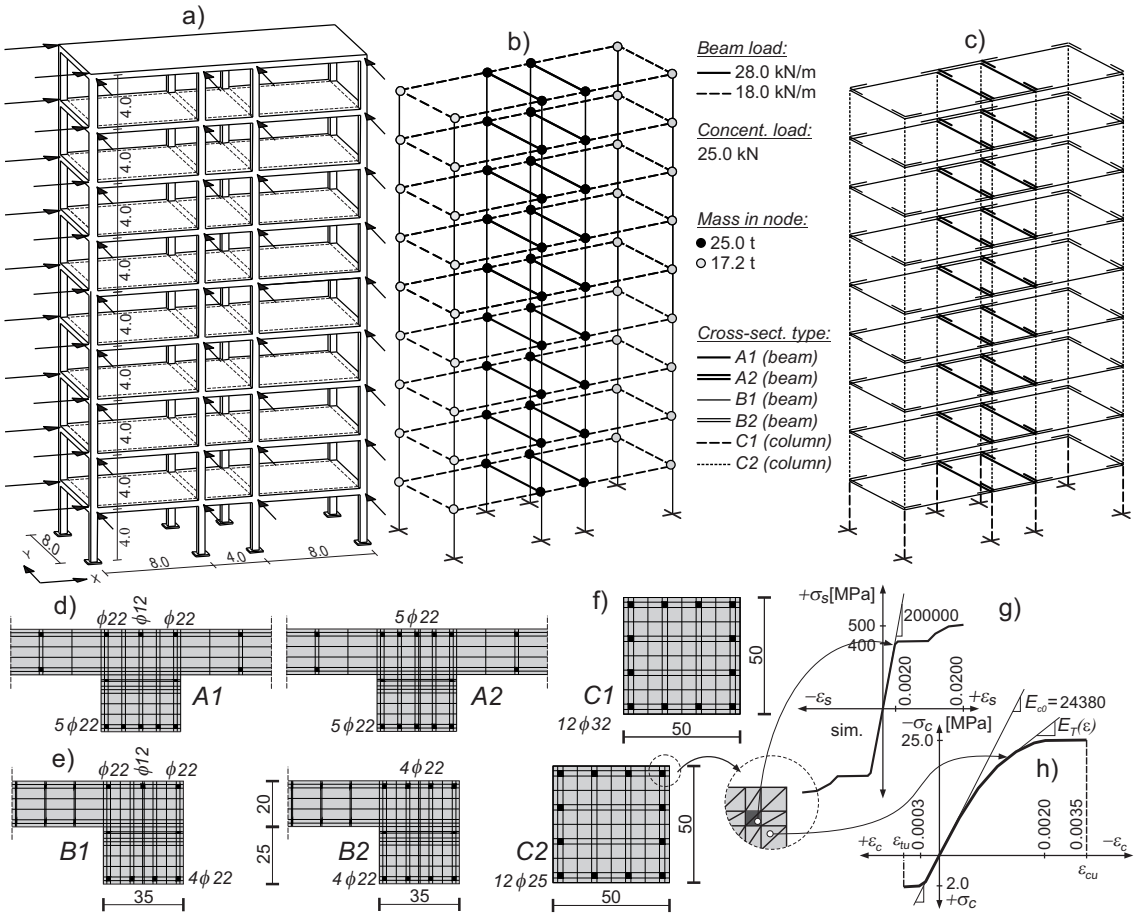

Figure 2: Example: a) Space frame; b) loading on beams and concentrated masses; c) labels of cross sections; d)-f) discretization of cross sections; g)-h) numerical model for steel and concrete.

By solving the linear dynamic analysis, eigenvectors are obtained $\boldsymbol{\phi}_i$, as well as periods T_i and modal masses m_{ei}, as shown in Table 1.

Load distribution and intensity of lateral forces are defined according to Equation 1. Thus defined shape of lateral loading vector is monotonically increased in nonlinear analysis, up to failure, i.e. achieving critical load factor. The sum of all horizontal forces gives failure force F_{fi} for the each eigen vector.

Vector	T_i [s]	m_{ei} [%]	m_{ei} [t]	F_{fi} [kN]
ϕ_1	2.298	79.87	1213.4	1330
ϕ_2	0.746	10.37	157.5	1530
ϕ_3	0.420	3.87	58.8	2035
ϕ_4	0.282	2.20	33.4	1770
ϕ_5	0.207	1.38	21.0	2490

Table 1: Properties of load vector for *x* direction.

Shape of the first vector in limit state and corresponding bearing capacity curve for *x* direction are shown on Figure 3.

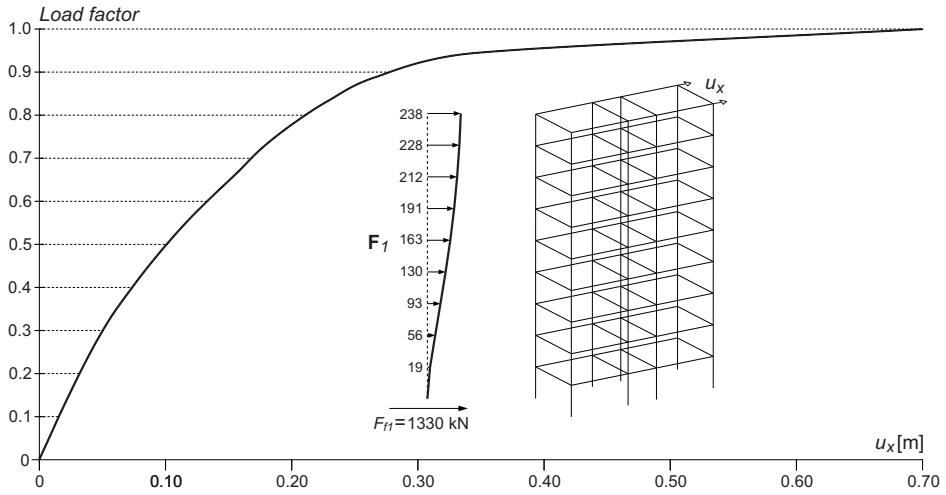

Figure 3: Capacity curve of vector ϕ_1 for *x* direction.

For the same direction *x*, conversion of capacity curve into ADRS format, determining the elasto-plastic equivalent, as well as limit (target) acceleration according to Eurocode 8 for the first mode, are all shown in Figure 4.

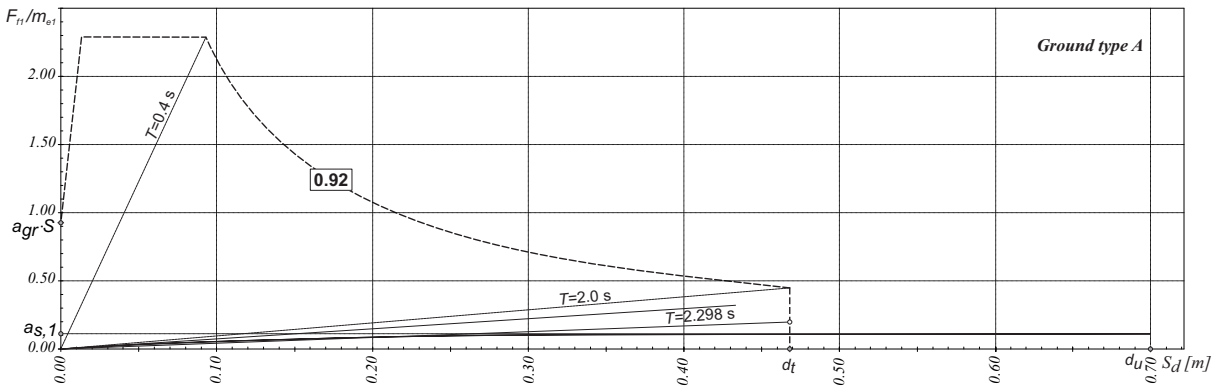

Figure 4: Computation of earthquake resistance for the first vector (F_1), for ground type *A*.

3.2 Determination of target acceleration for *x* direction

When searching for target acceleration, for assumed acceleration in the first step, assumed target acceleration obtained for the first vector is chosen, i.e. $a_{gr,1}$ = 0.92g. The same procedure is applied on other modes. Table 2 shows the procedure for trial method with result for minimal a_{gr} in case of target acceleration for linear combination. Obtained target acceleration has a value of $a_{gr,t}$ = 0.19g.

Figure 5 shows loading vector for all other participating modes, capacity curve as well as beginning of plastification and plastic hinge positions, for linear combination of modes. Early beginning of plastification is caused by loading in a way typical for pushover method, where gravity loading is set in the first phase, and in the second phase, horizontal loading is set. Hence, plastification begins immediately after start of the second phase - horizontal loading.

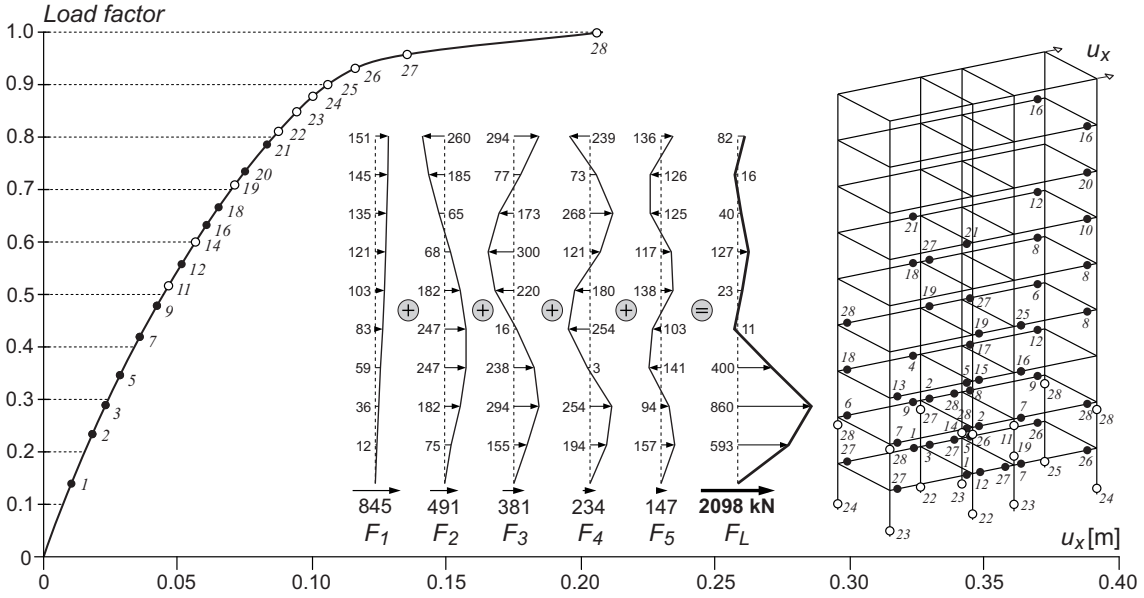

Figure 5: Capacity curve for linear combination of modes (*x* direction).

$a_{gr,i}$	$a_{s,1}$	F_1	$a_{s,2}$	F_2	$a_{s,3}$	F_3	$a_{s,4}$	F_4	$a_{s,5}$	F_5	ΣF_i	F_L	$F_L/\Sigma F_i$	δ_1	δ_2	δ_3	δ_4	δ_5
0.92	0.112	1330	0.923	1426	2.239	1292	2.700	886	3.161	651	5585	2681	0.48	0.121	1.003	2.434	2.935	3.436
0.50	0.107	1274	0.694	1072	1.428	824	1.749	574	1.858	383	4126	2476	0.60	0.214	1.388	2.856	3.498	3.716
0.20	0.073	869	0.448	692	0.689	398	0.750	246	0.750	155	2359	2123	0.90	0.365	2.240	3.445	3.750	3.750
0.19	0.071	845	0.318	491	0.660	381	0.713	234	0.713	147	2098	2098	**1.00**	0.374	1.674	3.474	3.753	3.753
0.18	0.068	809	0.307	474	0.623	359	0.675	221	0.675	139	2004	2164	1.08	0.378	1.706	3.461	3.750	3.750

Table 2: Target acceleration determination for linear combination (*x* direction).

Results for SRSS modal combination in *x* direction are shown in Table 3. Target acceleration is $a_{gr,t}$ = 0.25g. It is the minimal force in the base (1865 kN) does not correspond to target acceleration. Comparison of given target accelerations, gives the conclusion that linear combination is more unfavourable than SRSS combination because failure appears at lower target displacement.

$a_{gr,i}$	$a_{s,1}$	F_1	$a_{gr,i}/2$	$a_{s,2}$	F_2	$a_{s,3}$	F_3	$a_{s,4}$	F_4	$a_{s,5}$	F_5	ΣF_i	F_{SRSS}	$F_{SRSS}/\Sigma F_i$	δ_1	δ_2	δ_3	δ_4	δ_5
0.92	0.112	1330	0.46	0.651	1006	1.350	779	1.637	537	1.725	355	4010	2085	0.52	0.122	0.708	1.467	1.779	1.875
0.50	0.107	1274	0.25	0.391	604	0.845	488	0.938	308	0.938	193	2866	2064	0.72	0.214	0.782	1.690	1.876	1.876
0.30	0.093	1107	0.15	0.260	402	0.523	302	0.538	176	0.563	116	2103	2439	1.16	0.310	0.867	1.743	1.793	1.877
0.25	0.085	1011	0.125	0.225	348	0.442	255	0.469	154	0.469	97	1865	1865	**1.00**	0.340	0.900	1.768	1.876	1.876
0.20	0.073	869	0.10	0.182	281	0.354	204	0.375	123	0.375	77	1555	1368	0.88	0.365	0.910	1.770	1.875	1.875

Table 3: Target acceleration determination for SRSS combination (*x* direction).

Loading vector for each participating mode, capacity curve as well as beginning of plastification and plastic hinge positions, for SRSS combination of modes are shown in Figure 6.

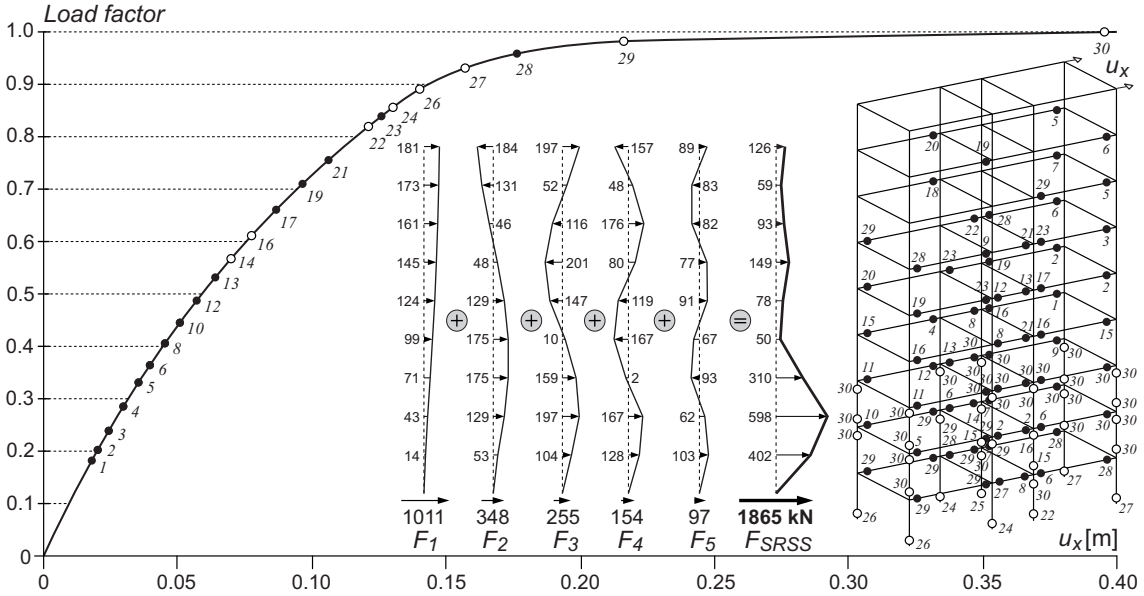

Figure 6: Capacity curve for SRSS combination (*x* direction).

3.3 Determination of target acceleration for *y* direction

Hereafter, results of analysis for *y* direction are presented. Properties of loading vector for each mode are shown in Table 4.

Vector	T_i [s]	m_{ei} [%]	m_{ei} [t]	F_{fi} [kN]
ϕ_1	2.715	78.91	1198.8	1410
ϕ_2	0.869	10.59	160.9	1735
ϕ_3	0.478	4.10	62.3	1965
ϕ_4	0.317	1.60	24.3	2340
ϕ_5	0.224	1.40	21.3	2435

Table 4: Properties of load vector for *y* direction.

Searching for target acceleration for linear combination in *y* direction is shown in Table 5. In searching for target acceleration, for assumed acceleration in the first step, assumed target acceleration obtained for the first vector is chosen, i.e. $a_{gr,1}$ = 1.05g. Obtained target acceleration has a value of $a_{gr,t}$=0.18g.

$a_{gr,i}$	$a_{s,1}$	F_1	$a_{s,2}$	F_2	$a_{s,3}$	F_3	$a_{s,4}$	F_4	$a_{s,5}$	F_5	ΣF_i	F_L	$F_L/\Sigma F_i$	δ_1	δ_2	δ_3	δ_4	δ_5
1.05	0.120	1410	0.917	1447	2.313	1413	3.900	928	3.606	754	5952	2619	0.44	0.114	0.873	2.203	3.714	3.434
0.40	0.097	1141	0.494	780	1.063	649	1.500	357	1.500	314	3240	2203	0.68	0.243	1.235	2.658	3.750	3.750
0.20	0.063	741	0.309	488	0.588	359	0.750	179	0.750	157	1923	1846	0.96	0.315	1.545	2.940	3.750	3.750
0.18	0.058	682	0.277	437	0.537	328	0.675	161	0.675	141	1749	1749	**1.00**	0.322	1.539	2.983	3.750	3.750
0.17	0.056	659	0.265	418	0.500	306	0.638	152	0.638	133	1667	1834	1.10	0.329	1.559	2.941	3.753	3.753

Table 5: Target acceleration determination for linear combination (*y* direction).

Loading vector for each participating mode, capacity curve for a linear combination as well as the sequence and place of the beginning of plastification and plastic hinge positions are shown in Figure 7.

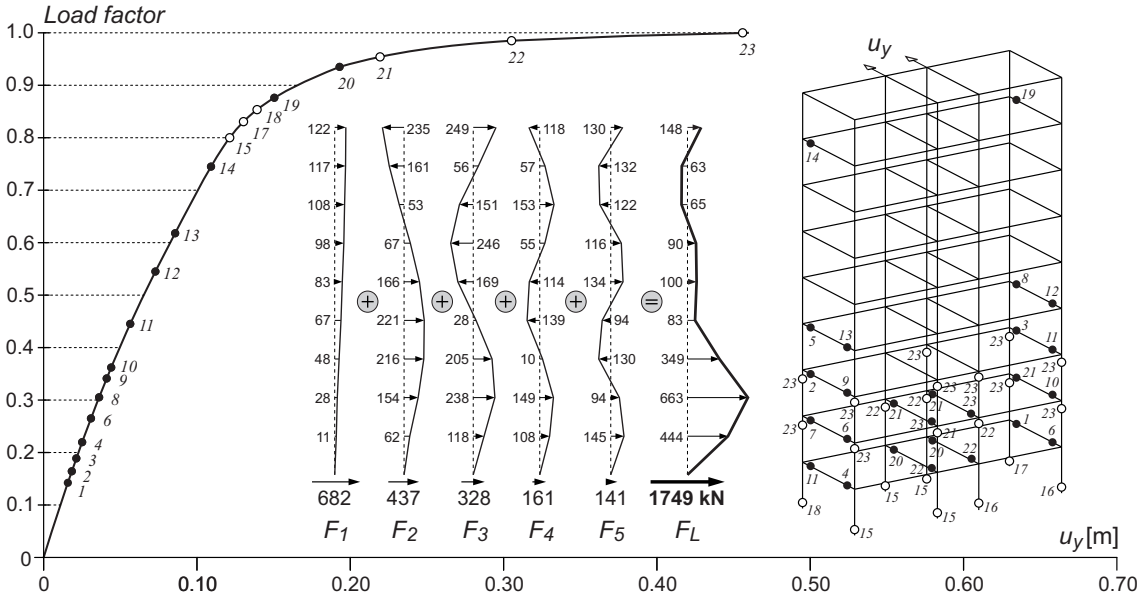

Figure 7: Capacity curve for linear combination (*y* direction).

Procedure of searching for target displacement in case of SRSS mode combination is shown in Table 6. Target acceleration is $a_{gr,t}$ = 0.245g. Linear combination has proven to be relevant *y* direction too, because the failure of structure appears at lower target acceleration ($a_{gr,t}$=0.18g) than target acceleration in case of SRSS mode combination ($a_{gr,t}$=0.245g).

$a_{gr,i}$	$a_{s,1}$	F_1	$a_{gr,i}/2$	$a_{s,2}$	F_2	$a_{s,3}$	F_3	$a_{s,4}$	F_4	$a_{s,5}$	F_5	ΣF_i	F_{SRSS}	$F_{SRSS}/\Sigma F_i$	δ_1	δ_2	δ_3	δ_4	δ_5
1.05	0.120	1410	0.525	0.610	963	1.300	794	1.968	468	1.879	393	4028	2175	0.54	0.114	0.581	1.238	1.874	1.790
0.40	0.097	1141	0.20	0.309	488	0.588	359	0.750	179	0.750	157	2323	1812	0.78	0.243	0.773	1.470	1.875	1.875
0.245	0.073	858	0.123	0.207	327	0.357	218	0.459	109	0.459	96	1608	1608	**1.00**	0.298	0.845	1.457	1.873	1.873
0.24	0.072	847	0.12	0.203	320	0.350	214	0.450	107	0.450	94	1582	1661	1.05	0.300	0.846	1.458	1.875	1.875
0.20	0.063	741	0.10	0.173	273	0.295	180	0.375	89	0.375	78	1362	1702	1.25	0.315	0.865	1.475	1.875	1.875

Table 6: Target acceleration determination for SRSS combination (*y* direction).

Loading vector for each participating mode, capacity curve as well as beginning of plastification and plastic hinge positions, for SRSS combination of modes is shown in Figure 8.

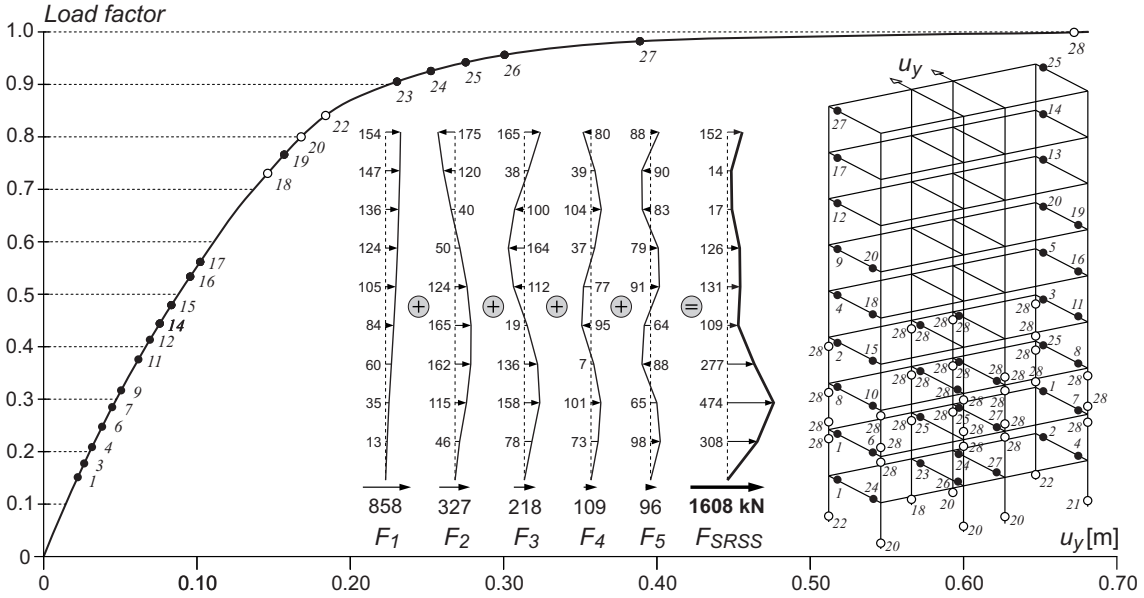

Figure 8: Capacity curve for SRSS combination (y direction).

4 APPEARANCE OF LINEAR (L) AND ROOT (SRSS) MODAL COMBINATION

The procedure that follows is intended to determine which of the specified combination of modes are likely to rally in the verification on the set of the following eight real earthquake accelerograms: Montenegro (Montenegro)-1979, Campano Lucano (Italy)-1980, Aigion (Greece)-1995, Olfus (Iceland)-2008, Calabria (Italy)-1978, Valnerina (Italy)-1979, Banja Luka (B&H)-1981 and Sicilia Orientale (Italy)-1990, all shown in Figure 9. Records of the earthquake accelerograms are taken from the European Strong-motion Database [19].

Verification of L and SRSS combination of modes on the linear and non-linear level of single degree of freedom system (SDOF) are taken as the obtained modes for observed 9-storey RC frames.

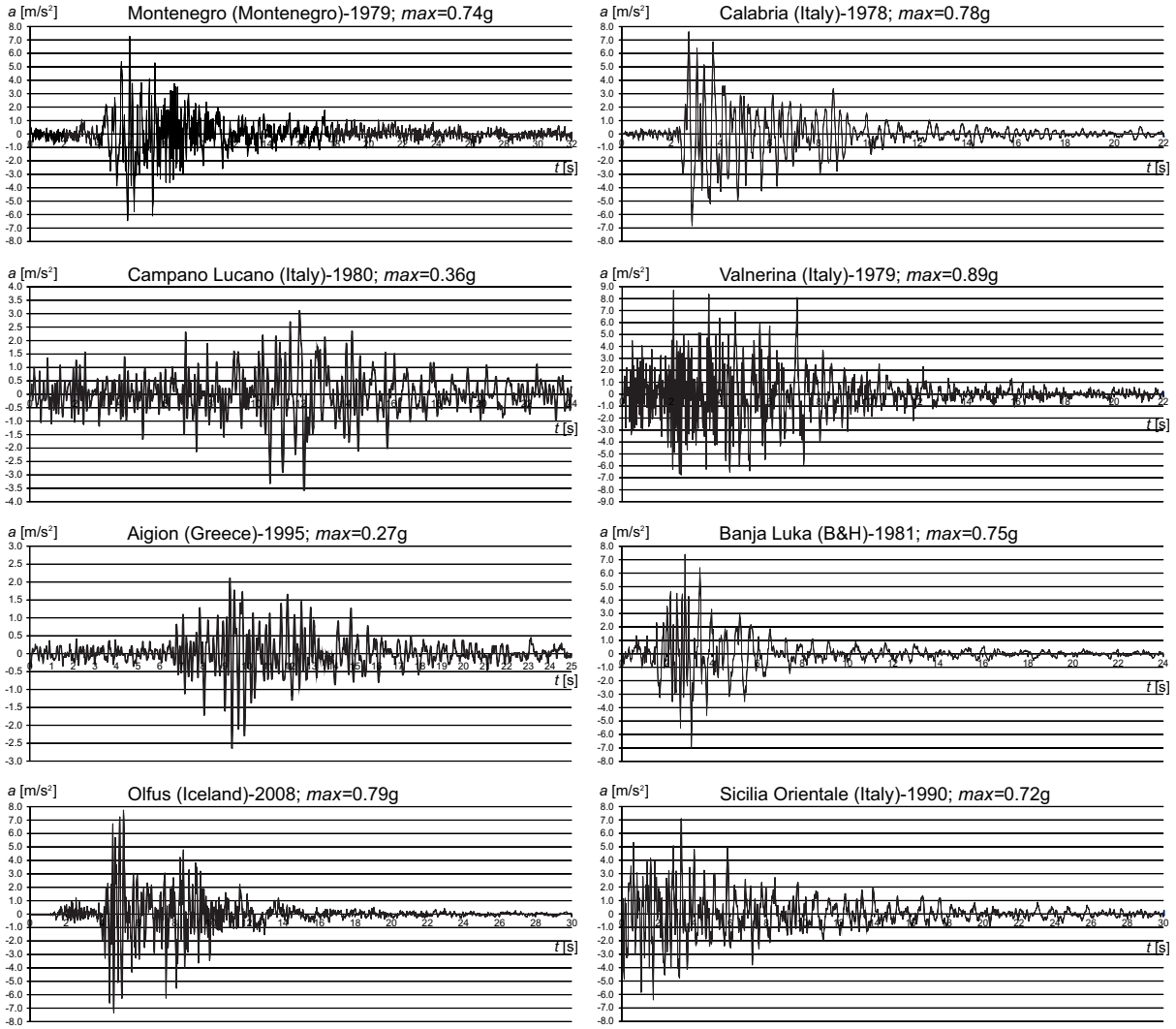

Figure 9: Eight real earthquake accelerograms.

Dynamic response of each SDOF is obtained by Newmark's average acceleration method. Numerical integration is written in computer program C++ according to the procedure described in [20].

4.1 Verification of L and SRSS combination of modes on the linear level

The 9-storey space RC frame from example in Figure 2 is analyzed. Shear forces in the cross section at the base of the calculation model (F_i) are calculated as a time function for each of the five eigen modes. Stiffness k of the linear SDOF is defined by the known period T_i and associated participating mass m_i corresponding to each own vector $\boldsymbol{\phi}_i$.

A relative measure of the force is introduced by which the greatest force of all modes ($|F_{max}|$) is equal to *1.00* and the others are relative to her.

Figure 10 shows a diagram of the shear forces in the cross section at the base of the calculation model (F_i) as a time function for all five eigen modes, for example of 9-storey RC frame loaded in the x direction by earthquake excitation Montenegro. It can be seen that in the relative scale of the force, the maximum amount of force of all five modes ($|F_{max}|$=689 kN) corresponds to a value *1.00*.

Maximum values of shear forces in the intersection at the base of the calculation model for all modes, which are shown in Tables 7 and 8, resulting from the action of eight real selected earthquake accelerogram records are obtained in an analogous way.

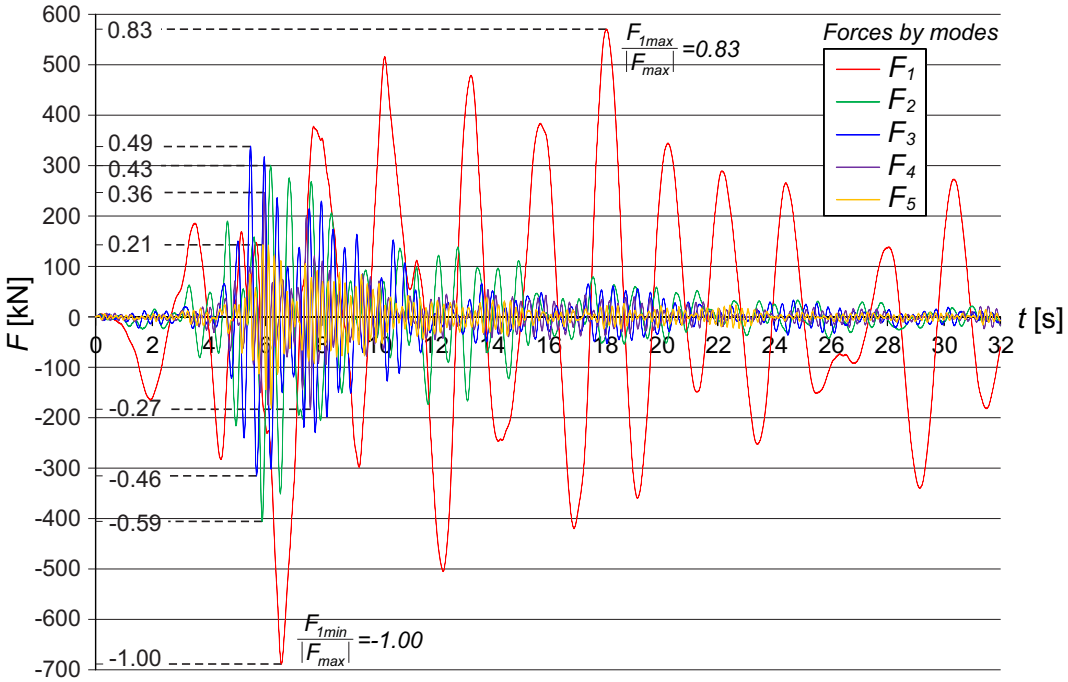

Figure 10: Shear forces in the cross section at the base of the calculation model of 9-storey RC frame for all five modes, as a time function of the earthquake excitation Montenegro for *x* direction.

Table 7 shows the results of analysis for the *x* and *y* directions, which presents the least favourable combination of simultaneous linear superposition of modes F_L as well as the least favourable combination of the square root of the sum of square of modes F_{SRSS}.

Montenegro **- 9-storey RC frame -** ***x*** **direction**						
F_{1max}	F_{2max}	F_{3max}	F_{4max}	F_{5max}	**for the same** ***t***	
0,83	0,43	0,49	0,36	0,21		
F_{1min}	F_{2min}	F_{3min}	F_{4min}	F_{5min}	F_L	-1,45
-1,00	-0,59	-0,46	-0,27	-0,26	F_{SRSS}	1,14

Campano Lucano **- 9-storey RC frame -** ***x*** **dir.**						
F_{1max}	F_{2max}	F_{3max}	F_{4max}	F_{5max}	**for the same** ***t***	
1,00	0,63	0,50	0,30	0,25		
F_{1min}	F_{2min}	F_{3min}	F_{4min}	F_{5min}	F_L	-1,36
-0,87	-0,47	-0,60	-0,25	-0,25	F_{SRSS}	1,14

Aigion **- 9-storey RC frame -** ***x*** **direction**						
F_{1max}	F_{2max}	F_{3max}	F_{4max}	F_{5max}	**for the same** ***t***	
0,90	0,52	0,51	0,84	0,40		
F_{1min}	F_{2min}	F_{3min}	F_{4min}	F_{5min}	F_L	-1,59
-1,00	-0,53	-0,59	-0,99	-0,35	F_{SRSS}	1,15

Olfus **- 9-storey RC frame -** ***x*** **direction**						
F_{1max}	F_{2max}	F_{3max}	F_{4max}	F_{5max}	**for the same** ***t***	
1,00	0,20	0,25	0,17	0,24		
F_{1min}	F_{2min}	F_{3min}	F_{4min}	F_{5min}	F_L	0,97
-0,92	-0,17	-0,22	-0,15	-0,21	F_{SRSS}	1,00

Calabria **- 9-storey RC frame -** ***x*** **direction**						
F_{1max}	F_{2max}	F_{3max}	F_{4max}	F_{5max}	**for the same** ***t***	
0,70	0,83	0,99	0,52	0,33		
F_{1min}	F_{2min}	F_{3min}	F_{4min}	F_{5min}	F_L	1,44
-0,67	-0,66	-1,00	-0,61	-0,36	F_{SRSS}	1,23

Valnerina **- 9-storey RC frame -** ***x*** **direction**						
F_{1max}	F_{2max}	F_{3max}	F_{4max}	F_{5max}	**for the same** ***t***	
0,83	0,65	0,37	0,27	0,15		
F_{1min}	F_{2min}	F_{3min}	F_{4min}	F_{5min}	F_L	1,35
-1,00	-0,72	-0,35	-0,28	-0,13	F_{SRSS}	1,09

Banja Luka **- 9-storey RC frame -** ***x*** **direction**						
F_{1max}	F_{2max}	F_{3max}	F_{4max}	F_{5max}	**for the same** ***t***	
0,75	1,00	0,31	0,20	0,17		
F_{1min}	F_{2min}	F_{3min}	F_{4min}	F_{5min}	F_L	-1,36
-0,53	-0,93	-0,37	-0,24	-0,19	F_{SRSS}	1,08

Sicilia Orientale **- 9-storey RC frame -** ***x*** **dir.**						
F_{1max}	F_{2max}	F_{3max}	F_{4max}	F_{5max}	**for the same** ***t***	
0,88	0,75	0,47	0,28	0,25		
F_{1min}	F_{2min}	F_{3min}	F_{4min}	F_{5min}	F_L	-1,54
-1,00	-0,86	-0,48	-0,25	-0,23	F_{SRSS}	1,21

Montenegro **- 9-storey RC frame -** ***y*** **direction**						
F_{1max}	F_{2max}	F_{3max}	F_{4max}	F_{5max}	**for the same** ***t***	
0,71	0,25	0,58	0,16	0,22		
F_{1min}	F_{2min}	F_{3min}	F_{4min}	F_{5min}	F_L	-1,06
-1,00	-0,39	-0,65	-0,14	-0,21	F_{SRSS}	1,00

Campano Lucano **- 9-storey RC frame -** ***y*** **dir.**						
F_{1max}	F_{2max}	F_{3max}	F_{4max}	F_{5max}	**for the same** ***t***	
0,90	1,00	0,58	0,18	0,23		
F_{1min}	F_{2min}	F_{3min}	F_{4min}	F_{5min}	F_L	1,72
-0,95	-0,80	-0,72	-0,25	-0,21	F_{SRSS}	1,11

Aigion **- 9-storey RC frame -** ***y*** **direction**						
F_{1max}	F_{2max}	F_{3max}	F_{4max}	F_{5max}	**for the same** ***t***	
0,97	0,32	0,39	0,45	0,27		
F_{1min}	F_{2min}	F_{3min}	F_{4min}	F_{5min}	F_L	-1,35
-1,00	-0,33	-0,40	-0,50	-0,25	F_{SRSS}	1,03

Olfus **- 9-storey RC frame -** ***y*** **direction**						
F_{1max}	F_{2max}	F_{3max}	F_{4max}	F_{5max}	**for the same** ***t***	
0,94	0,29	0,32	0,20	0,41		
F_{1min}	F_{2min}	F_{3min}	F_{4min}	F_{5min}	F_L	1,06
-1,00	-0,23	-0,33	-0,18	-0,34	F_{SRSS}	1,00

Calabria **- 9-storey RC frame -** ***y*** **direction**						
F_{1max}	F_{2max}	F_{3max}	F_{4max}	F_{5max}	**for the same** ***t***	
0,33	0,49	1,00	0,60	0,31		
F_{1min}	F_{2min}	F_{3min}	F_{4min}	F_{5min}	F_L	1,16
-0,25	-0,38	-0,93	-0,55	-0,28	F_{SRSS}	1,04

Valnerina **- 9-storey RC frame -** ***y*** **direction**						
F_{1max}	F_{2max}	F_{3max}	F_{4max}	F_{5max}	**for the same** ***t***	
0,96	0,64	0,35	0,21	0,15		
F_{1min}	F_{2min}	F_{3min}	F_{4min}	F_{5min}	F_L	1,46
-1,00	-0,50	-0,41	-0,21	-0,13	F_{SRSS}	1,18

Banja Luka **- 9-storey RC frame -** ***y*** **direction**						
F_{1max}	F_{2max}	F_{3max}	F_{4max}	F_{5max}	**for the same** ***t***	
0,79	1,00	0,76	0,29	0,29		
F_{1min}	F_{2min}	F_{3min}	F_{4min}	F_{5min}	F_L	-1,54
-0,50	-0,84	-0,73	-0,28	-0,30	F_{SRSS}	1,12

Sicilia Orientale **- 9-storey RC frame -** ***y*** **dir.**						
F_{1max}	F_{2max}	F_{3max}	F_{4max}	F_{5max}	**for the same** ***t***	
0,74	0,65	0,54	0,27	0,35		
F_{1min}	F_{2min}	F_{3min}	F_{4min}	F_{5min}	F_L	1,48
-1,00	-0,58	-0,61	-0,21	-0,33	F_{SRSS}	1,03

Table 7: Comparison of linear (L) and root (SRSS) combination of modes for 9-storey RC frame on linear level.

Presented results of dynamic response of linear system according to Table 7 shows that the linear combination of modes F_L is frequently unfavourable than the square root of sum of square combinations of modes F_{SRSS}.

4.2 Verification of L and SRSS combination of modes on the non-linear level

Non-linear levels is achieved so that each mode is treated as a nonlinear SDOF. Non-linear cyclic properties of SDOF are generated from the corresponding capacity curve as shown in Figure 11 and equation (6).

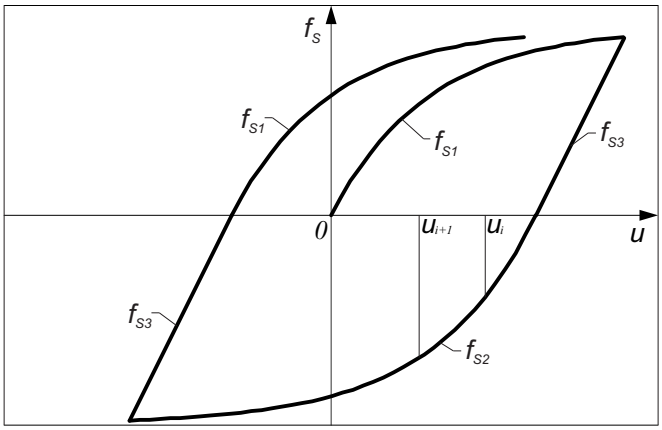

Figure 11: Cyclic capacity curve for the non-linear system.

Figure corresponding functions are defined in such a way to have the following analytical form:

$$f_{s1} = A\left(1 - e^{-\frac{u-B}{C}}\right) + D$$
$$f_{s2} = -A\left(1 - e^{\frac{u-B}{C}}\right) + D \tag{6}$$
$$f_{s3} = \frac{A}{C}(u - B) + D$$

The function f_{S1} corresponds to capacity curve for each mode. With it the coefficients A and C are defined in the expression (6). The function f_{S3} is linear and the slope of its corresponds to initial stiffness of SDOF. Coefficients B and D are calculated in each time step and by them translation of functions f_{S1} and f_{S2} to the axis u for the coefficient B and the axis f_S for the coefficient D are defined.

Table 8 shows the results of the analysis of non-linear SDOF for the x and y directions, which presents the least favourable combination of simultaneous linear superposition of modes F_L as well as the least favourable combination of the square root of the sum of square of modes F_{SRSS}.

Montenegro **- 9-storey RC frame -** ***x*** **direction**						
F_{1max}	F_{2max}	F_{3max}	F_{4max}	F_{5max}	**for the same** ***t***	
0,69	0,92	0,69	0,52	0,32		
F_{1min}	F_{2min}	F_{3min}	F_{4min}	F_{5min}	F_L	-2,02
-0,78	-1,00	-0,66	-0,60	-0,34	F_{SRSS}	1,31
Campano Lucano **- 9-storey RC frame -** ***x*** **dir.**						
F_{1max}	F_{2max}	F_{3max}	F_{4max}	F_{5max}	**for the same** ***t***	
0,73	0,95	0,67	0,33	0,27		
F_{1min}	F_{2min}	F_{3min}	F_{4min}	F_{5min}	F_L	-1,68
-0,68	-1,00	-0,65	-0,36	-0,29	F_{SRSS}	1,32
Aigion **- 9-storey RC frame -** ***x*** **direction**						
F_{1max}	F_{2max}	F_{3max}	F_{4max}	F_{5max}	**for the same** ***t***	
0,89	0,92	0,99	1,00	0,85		
F_{1min}	F_{2min}	F_{3min}	F_{4min}	F_{5min}	F_L	2,12
-0,98	-0,89	-0,99	-0,85	-0,93	F_{SRSS}	1,41
Olfus **- 9-storey RC frame -** ***x*** **direction**						
F_{1max}	F_{2max}	F_{3max}	F_{4max}	F_{5max}	**for the same** ***t***	
0,96	0,71	1,00	0,44	0,25		
F_{1min}	F_{2min}	F_{3min}	F_{4min}	F_{5min}	F_L	1,92
-0,97	-0,75	-0,90	-0,38	-0,26	F_{SRSS}	1,15
Calabria **- 9-storey RC frame -** ***x*** **direction**						
F_{1max}	F_{2max}	F_{3max}	F_{4max}	F_{5max}	**for the same** ***t***	
0,40	1,00	0,63	0,35	0,28		
F_{1min}	F_{2min}	F_{3min}	F_{4min}	F_{5min}	F_L	1,29
-0,42	-0,93	-0,56	-0,34	-0,26	F_{SRSS}	1,02
Valnerina **- 9-storey RC frame -** ***x*** **direction**						
F_{1max}	F_{2max}	F_{3max}	F_{4max}	F_{5max}	**for the same** ***t***	
0,79	0,78	0,59	0,44	0,39		
F_{1min}	F_{2min}	F_{3min}	F_{4min}	F_{5min}	F_L	-1,49
-1,00	-0,79	-0,56	-0,48	-0,37	F_{SRSS}	1,13
Banja Luka **- 9-storey RC frame -** ***x*** **direction**						
F_{1max}	F_{2max}	F_{3max}	F_{4max}	F_{5max}	**for the same** ***t***	
0,59	1,00	0,56	0,47	0,32		
F_{1min}	F_{2min}	F_{3min}	F_{4min}	F_{5min}	F_L	-2,04
-0,41	-1,00	-0,55	-0,58	-0,35	F_{SRSS}	1,08
Sicilia Orientale **- 9-storey RC frame -** ***x*** **dir.**						
F_{1max}	F_{2max}	F_{3max}	F_{4max}	F_{5max}	**for the same** ***t***	
0,75	0,90	1,00	0,42	0,25		
F_{1min}	F_{2min}	F_{3min}	F_{4min}	F_{5min}	F_L	2,34
-0,93	-0,93	-0,99	-0,39	-0,25	F_{SRSS}	1,37

Montenegro **- 9-storey RC frame -** ***y*** **direction**						
F_{1max}	F_{2max}	F_{3max}	F_{4max}	F_{5max}	**for the same** ***t***	
0,77	0,64	0,67	0,23	0,29		
F_{1min}	F_{2min}	F_{3min}	F_{4min}	F_{5min}	F_L	-1,49
-1,00	-0,60	-0,64	-0,24	-0,33	F_{SRSS}	1,13
Campano Lucano **- 9-storey RC frame -** ***y*** **dir.**						
F_{1max}	F_{2max}	F_{3max}	F_{4max}	F_{5max}	**for the same** ***t***	
0,93	0,90	0,71	0,15	0,33		
F_{1min}	F_{2min}	F_{3min}	F_{4min}	F_{5min}	F_L	-2,14
-1,00	-0,87	-0,68	-0,18	-0,36	F_{SRSS}	1,34
Aigion **- 9-storey RC frame -** ***y*** **direction**						
F_{1max}	F_{2max}	F_{3max}	F_{4max}	F_{5max}	**for the same** ***t***	
0,74	0,63	0,89	0,13	0,42		
F_{1min}	F_{2min}	F_{3min}	F_{4min}	F_{5min}	F_L	1,93
-0,75	-0,58	-1,00	-0,14	-0,47	F_{SRSS}	1,13
Olfus **- 9-storey RC frame -** ***y*** **direction**						
F_{1max}	F_{2max}	F_{3max}	F_{4max}	F_{5max}	**for the same** ***t***	
0,96	0,66	0,53	0,27	0,24		
F_{1min}	F_{2min}	F_{3min}	F_{4min}	F_{5min}	F_L	1,53
-1,00	-0,65	-0,57	-0,25	-0,25	F_{SRSS}	1,06
Calabria **- 9-storey RC frame -** ***y*** **direction**						
F_{1max}	F_{2max}	F_{3max}	F_{4max}	F_{5max}	**for the same** ***t***	
0,33	0,82	0,99	0,25	0,40		
F_{1min}	F_{2min}	F_{3min}	F_{4min}	F_{5min}	F_L	-1,58
-0,24	-0,89	-1,00	-0,20	-0,36	F_{SRSS}	1,35
Valnerina **- 9-storey RC frame -** ***y*** **direction**						
F_{1max}	F_{2max}	F_{3max}	F_{4max}	F_{5max}	**for the same** ***t***	
0,91	0,65	0,70	0,61	0,28		
F_{1min}	F_{2min}	F_{3min}	F_{4min}	F_{5min}	F_L	-2,31
-1,00	-0,71	-0,69	-0,59	-0,28	F_{SRSS}	1,33
Banja Luka **- 9-storey RC frame -** ***y*** **direction**						
F_{1max}	F_{2max}	F_{3max}	F_{4max}	F_{5max}	**for the same** ***t***	
0,44	0,90	0,47	0,25	0,41		
F_{1min}	F_{2min}	F_{3min}	F_{4min}	F_{5min}	F_L	1,40
-0,36	-1,00	-0,51	-0,29	-0,45	F_{SRSS}	1,08
Sicilia Orientale **- 9-storey RC frame -** ***y*** **dir.**						
F_{1max}	F_{2max}	F_{3max}	F_{4max}	F_{5max}	**for the same** ***t***	
0,69	1,00	0,68	0,28	0,30		
F_{1min}	F_{2min}	F_{3min}	F_{4min}	F_{5min}	F_L	-2,13
-0,87	-0,96	-0,63	-0,30	-0,26	F_{SRSS}	1,32

Table 8: Comparison of linear (L) and root (SRSS) combination of modes for 9-storey RC frame on non-linear level.

The presented results for the non-linear dynamic response of the system according to Table 8 shows that the linear combination of modes F_L in all cases is considerably unfavourable than the square root of sum of square combinations of modes F_{SRSS}.

5 CONCLUSIONS

This paper describes a procedure for determining the target acceleration, defined as the minimum ground acceleration that leads to ultimate limit state of construction using multi-modal pushover method, which represents the lowest earthquake resistance.

The procedure is based on the successive application of non-linear static analysis in multi-modal pushover method and successive trials in searching for targeted acceleration which has all the characteristics of an envelope principle.

Based on the results of presented examples, following conclusion is made:

- Influence of higher modes, especially the second and third mode is very significant.
- Target ground acceleration, respectively the lowest limit acceleration is not necessarily generated by the smallest lateral force in the base. Thereat minimal limit acceleration is lower than limit acceleration of each mode independently.
- Linear combination is more relevant because of lower target acceleration than the one obtained by SRSS combination of modes.
- The shape of general failure vector associated to the target acceleration differs significantly from the shape of the first vector loads and shape of loads with constant acceleration by height of structure contained in EN 1998.
- Appearance of linear combination (L) and square root of sum of square combination of modes (SRSS), tested for the actual series of real seismic records on the linear and nonlinear level confirms that the linear combination is more probable than combinations of square root of sum of square of modes.
- Multi-mode pushover method a priori assumes that in the real earthquake action all relevant modes are activated.
- Irrespective of the method of combining modes, the practical application of multimodal approach show that the safety/reliability of the observed RC frame are lower than that indicated by criteria for the target displacement, in accordance with Eurocode 8 (Annex B).
- Inclusion of higher modes, in presented examples, decreases the limit ground acceleration by more than two times, which is significantly less favourable than requirements for reserves in the capacity curve of 150% in relation to the target displacement of the peak of structure, i.e. target displacement criteria.

REFERENCES

[1] European Committee for Standardization (CEN): EN 1998-1. Eurocode 8: Design of Structures for earthquake resistance – Part 1: General rules, seismic actions and rules for buildings, Brussels, Belgium, 2004.

[2] ATC, Seismic evaluation and retrofit of concrete buildings, ATC-40 Report, *Applied Technology Council*, Redwood City, California, 1996.

[3] ATC, Improvement of nonlinear static seismic analysis procedures, FEMA 440 Report, *Applied Technology Council*, Redwood City, California, 2005.

[4] M. Saiidi, M.A. Sozen, Simple Nonlinear Seismic Analysis of R/C Structures, *Journal of the Structural Division*, **107**, 937-953, 1981.

[5] P. Fajfar, M. Fischinger, Non-linear seismic analysis of RC buildings: Implications of a case study, *European Earthquake Engineering*, **1**, 31-43, 1987.

[6] P. Fajfar, M. Fischinger, N2 – a method for non-linear seismic analysis of regular buildings, *Proc. 9th world conf. Earthquake eng.*, Tokyo, Kyoto, **5**, 111-116, 1988.

[7] P. Fajfar, P. Gašperšič, The N2 method for the seismic damage analysis for RC buildings, *Earthquake Engineering & Structural Dynamics*, **25**, 23–67, 1996.

[8] P. Fajfar, A Nonlinear Analysis Method for Performance Based Seismic Design, *Earthquake Spectra*, **16**, 573-592, 2000.

[9] N.D. Lagaros, M. Fragiadakis, Evaluation of ASCE-41, ATC-40 and N2 static pushover methods based on optimally designed buildings, *Soil Dynamics and Earthquake Engineering*, **31**, 77–90, 2011.

[10] A.K. Chopra, R.K. Goel, A modal pushover analysis procedures for estimating seismic demands for buildings, *Earthquake Engineering & Structural Dynamics*, **31**, 561–582, 2002.

[11] Y. Jiang, G. Li, D. Yang, A modified approach of energy balance concept based multimode pushover analysis to estimate seismic demands for buildings, *Engineering Structures*, **32**, 1272–1283, 2010.

[12] K.K. Sasaki, S.A. Freeman, T.F. Paret, Multi-mode pushover procedure (MMP) - a method to identify the effects of higher modes in a pushover analysis, *Proceedings of 6th U.S. National Conference on Earthquake Eng*ineering, Seattle (Washington), 1998.

[13] E. Kalkan, S.K. Kunnath, Assessment of current nonlinear static procedures for seismic evaluation of buildings, *Engineering Structures*, **29**, 305–316, 2007.

[14] A.K. Chopra, R.K. Goel, C. Chintanapakdee, Evaluation of a modified MPA procedure assuming higher modes as elastic to estimate seismic demands, *Earthquake Spectra*, **20**, 757-778, 2004.

[15] R.K. Goel, A.K. Chopra, Role of higher-"mode" pushover analyses in seismic analysis of buildings, *Earthquake Spectra*, **21**, 1027-1041, 2005.

[16] K. Shakeri, M. Mohebbi, Single-run modal pushover procedure based on the modal shear and moment in the stories, *Proceedings of 14th European Conference on Earthquake Eng*ineering, Ohrid, Republic of Macedonia, 6199-6207, 2010.

[17] B. Trogrlić, A. Mihanović, The comparative body model in material and geometric nonlinear analysis of space R/C frames, *Engineering Computations*, **25**, 155-171, 2008.

[18] B. Trogrlić, A. Mihanović, Ž. Nikolić, Modified Modal Pushover Analysis of RC Frames, *fib Symposium Prague 2011, Concrete engineering for excellence and efficiency, Proceedings*, Publisher: Czech Concrete Society (CBS) / Czech fib National Member Group, **2**, 95-98, 2011.

[19] http://www.isesd.hi.is, The European Strong-motion database, 04.04.2012.

[20] A.K. Chopra, *Dynamics of structures: Theory and Applications to Earthquake Engineering, University of California at Berkeley, Third Edition*, Prentice Hall, 2007.